Section 1   Cover page

Completed Research Report

การอัดตัวของหินดินดานตามลำดับขั้นชั้นกาลเวลาทางธรณีวิทยา

Compaction of Shales Based on Geological Time Sequences

Avirut Puttiwongrak, Ph.D. (Engineering)

บทคัดย่อ

ปัจจัยหลักของการบดอัดตัวของหินดินดานตามธรรมชาติคือการบดอัดทางกลศาสตร์ กล่าวคือ การบดอัดด้วยน้ำหนักกดทับหรืออีกนัยหนึ่งคือความลึกที่เพิ่มขึ้นจากการกดทับ อย่างไรก็ดีกราฟแสดงการบดอัดตัวของหินดินดานแสดงถึงแนวโน้มของข้อมูลที่กระจัดกระจาย และยังไม่สามารถกำหนดกราฟตัวแทนของการบดอัดตัวของหินดินดานได้ในปัจจุบัน นอกจากนี้ การกระจายตัวของข้อมูลการบดอัดตัวของหินดินดานยังไม่มีคำอธิบายและหาข้อสรุปถึงปัจจัย ของการกระจายตัวของข้อมูล งานวิจัยนี้มีวัตถุประสงค์เพื่อแสดงถึงความสำคัญของปัจจัยทาง ชั้นกาลเวลาทางธรณีและกำหนดสมการทางคณิตศาสตร์สำหรับการบดอัดตัวของหินดินดานที่ แสดงความสัมพันธ์ของค่าความพรุนของหินดินดาน ความลึกจากการกดทับ และชั้นกาลเวลา ทางธรณีของหินดินดาน ผลการวิจัยพบว่าชั้นกาลเวลาทางธรณีสามารถใช้อธิบายการกระจาย ตัวของข้อมูลการบดอัดของหินดินดาน เส้นกราฟที่ถูกวาดขึ้นจากสมการทางคณิตศาสตร์ที่ถูก คิดขึ้นในงานวิจัยนี้สามารถเป็นตัวแทนของข้อมูลการบดอัดของหินดินดานตามชั้นกาลเวลาทาง ธรณี ด้วยเหตุนี้จึงสามารถกล่าวได้ว่าปัจจัยการบดอัดทางกลศาสตร์ (คำนึงถึงเพียงความสัมพันธ์ แค่ค่าความพรุนของหินดินดานและความลึกจากการกดทับ) ไม่ใช่ปัจจัยหลักของการบดอัดตัว ของหินดินดานแต่เพียงปัจจัยเดียว ชั้นกาลเวลาทางธรณีเป็นอีกหนึ่งปัจจัยที่สำคัญที่จะต้อง คำนึงถึงสำหรับการศึกษาเรื่องการบดอัดตัวของหินดินดาน

ABSTRACT

Assembled compaction curves of mudrocks, including shales, (Skemption, 1944; Engelhardt and Gaida, 1963; Miyazaki, 1966; Meade, 1966; Baldwin and Butler, 1985; Dzevanshir et al., 1986; Mondol et al., 2007) have revealed that only mechanical compaction (compaction processes as a function of effective stress or burial depth) cannot explain variations of compaction curves. Time or geologic age has been studied to be an important factor to influence on shale compactions (Terzaghi, 1925, 1943; Versluys, 1927; McCoy and Keyte, 1934; Weatherby and Faust, 1935; Van Olphen, 1963; Burst, 1969, Dzevanshir et al., 1986), especially at shallow part of compaction processes. Consequently, this study shows an effect of time on shale compaction curves and we set up mathematic equation that can draw shale compaction curves with consideration of time. Finally, the study can help us to understand the mechanism of shale compactions, especially at the shallow part which is dominated by the mechanical compaction.

Section 2   Research Details

Project Name:

(English)   Compaction of Shales Based on Geological Time Sequences

(Thai)   การอัดตัวของหินดินดานตามลำดับขั้นชั้นกาลเวลาทางธรณีวิทยา

Person in Chanrge of Project

- Project Learder

Name-Surname	Dr. Avirut Puttiwongrak (ดร. อวิรุทธิ์ พุฒิวงศ์รักษ์)
Qualification	D.Phil. in Environment and Resource System Engineering Kyoto University, Japan
Position	Lecturer
Institute	Interdisciplinary Graduate School of Earth System Science and Andaman Natural Disaster Management (ESSAND) Prince of Songkla University Phuket Campus Kathu, Phuket, 83120 Tel. 080-2191411 Email: puttiwongrak_a@live.com

- Project Adviser (Liaison)

Name-Surname	Assoc. Prof. Dr. Pham Huy Giao
Position	Associate Professor Coordinator, Geotechnical and Earth Resource Engineering Coordinator, Geosystem Exploration and Petroleum Geoengineering Asian Institute of Technology, Thailand
Institute	Geotechnical and Earth Resource Engineering Asian Institute of Technology, Thailand

- Main Institute

  Interdisciplinary Graduate School of Earth System Science and Andaman Natural Disaster Management (ESSAND)

  Prince of Songkla University Phuket Campus

  Kathu Phuket 83120 Tel. 076-276-432

- Supporting Instutitue

  1) Prince of Songkla University

  2) Asian Institute of Technology

  3) Department of Mineral Fuel

CONTENT

LIST OF FIGURES

LIST OF TABLES

Acknowledgements

I have taken efforts in this research project. However, it would not have been possible without the kind support and help of many individuals and organizations. I would like to extend my sincere thanks to all of them.

I am highly indebted to Assoc.Prof.Dr. Pham Huy Giao, AIT, for guidance and constant supervision as well as for providing necessary information regarding the project and also for his support in completing the project.

I am obliged to DMF (Department of Mineral Fuels), Thailand, for their supports and valuable information in order to finish this project. I am grateful for their cooperation during the period of the project. I would like to express my special gratitude and thanks to their staffs for giving me such attention and time.

My thanks and appreciations also go to staff members of ESSAND, Prince of Songkla University Phuket campus, in developing the project and people who have willingly helped me out with their abilities.

Lastly, I would like to thank to RDO (Research and Development Office), Prince of Songkla University, for providing me the research budget and a good opportunity without which this project would not be possible.

Abstract

Assembled compaction curves of mudrocks, including shales, (Skemption, 1944; Engelhardt and Gaida, 1963; Miyazaki, 1966; Meade, 1966; Baldwin and Butler, 1985; Dzevanshir et al., 1986; Mondol et al., 2007) have revealed that only mechanical compaction (compaction processes as a function of effective stress or burial depth) cannot explain variations of compaction curves. Time or geologic age has been studied to be an important factor to influence on shale compactions (Terzaghi, 1925, 1943; Versluys, 1927; McCoy and Keyte, 1934; Weatherby and Faust, 1935; Van Olphen, 1963; Burst, 1969, Dzevanshir et al., 1986), especially at shallow part of compaction processes. Consequently, this study shows an effect of time on shale compaction curves and we set up mathematic equation that can draw shale compaction curves with consideration of time. Finally, the study can help us to understand the mechanism of shale compactions, especially at the shallow part which is dominated by the mechanical compaction.

1. Introduction

Effect of time or geologic age has been studied to be an important factor to influence on shale compactions for a very long time (Terzaghi, 1925, 1943; Versluys, 1927; McCoy and Keyte, 1934; Weatherby and Faust, 1935; Van Olphen, 1963; Burst, 1969, Dzevanshir et al., 1986). Terzaghi (1925) discussed the primitive expression of his compaction equation. He considered compaction in term of excess pore pressure of soils and relaxation of the excess pressure in time. Versluys (1927) discussed effective processes in compaction of clay, calculated compaction pressure, and he stated that time factor relates to the escape of water, which was also considered by Terzaghi. McCoy and Keyte (1934) studied on the expulsion of enormous quantities of water from compacting muds and raise doubts to the existence of a definite relation between overburden and density of shales. They confirmed that geological age may also be an important factor in controlling density. An evidence of seismograph work, it is known that, in argillaceous sediments, the velocity of seismic waves in general increases with rock density. Increasing water content, on the other hands, tends to diminish velocity. Both of these factors are usually dependent on degree of compaction. Weatherby and Faust (1935) have supplied data on the increase of seismic velocities with geologic age. However, they ignored effects of uplift and erosions. Van Olphen (1963) studied on clay mineral dehydration and concluded that many clay lattices in Paleozoic and older Tertiary sediments appear to have been dehydrated completely under normal compaction. In contrast, partial dehydration has also been observed in relatively young sediments. Because of the paucity of fully swelling clay material in Paleozoic and older Tertiary rocks and its abundance in young sediments, clay hydration state is a function of geologic age.

Burst (1969) is a pioneer to study effect of time on compaction processes quantitatively. He demonstrated his plots between porosity and geologic time based on Manger (1963)'s data of mudrocks (Manger reported only data without physical discussion). Burst (1969) suggested that the porosity of mudrocks tend to decline as a function of increasing time (Fig. 1.1). However, his plot was not clear because he only plotted ranges of porosities with times, and depths (or age range of sample) were not specified. Consequently, this research would propose a mathematic equation of shale campaction would be proposed based on geological time sequences and would reveal an effect of the time on shale compactions.
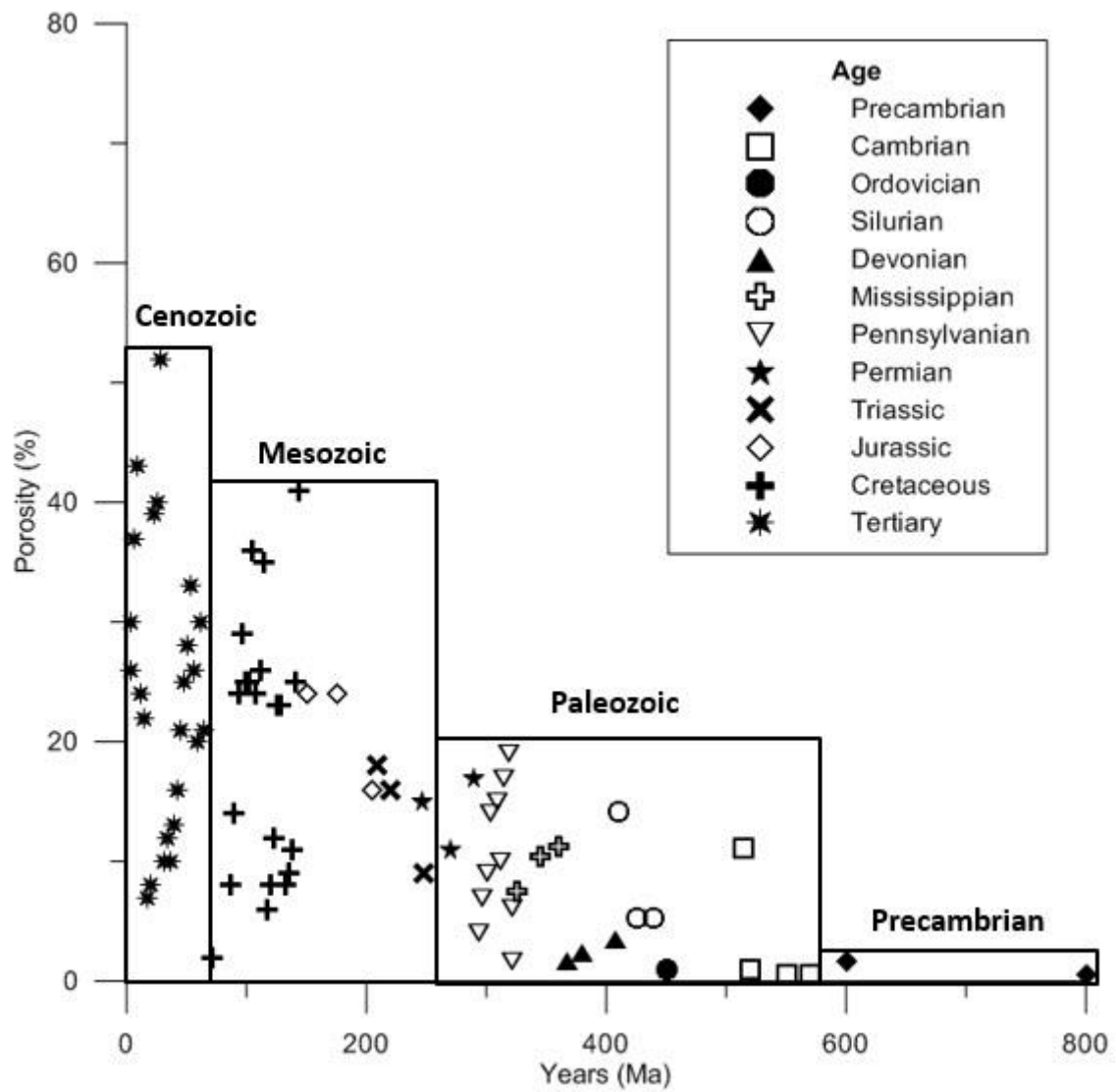
Fig. 1.1 Porosity-Geological time plots of shale compactioin data re-contrucuted from Burst (1969)

2. Objective

To research sequences of geological time on shale compaction curves and set up mathematic equation that can draw shale compaction curves with consideration of geological time. Finally, the research can help to understand the mechanism of shale compactions, especially at the shallow part which is dominated by the mechanical compaction.

3. Literature Review

Geological time is an important factor to influence the compaction as well as overburden. Time after deposition of mud promotes its compaction. Effect of geological time on the compaction is far more difficult for us to analyze than overburden. It is because an experiment is impossible for geological time. Normally, the processes of compaction of sediments are very slow, therefore a differential equation of excess pore pressure considering with time and depth proposed by Terzaghi (1925, 1943) and slow compaction model of Folwer and Yang (1998)'s differential equation can be analysed and solved. A mathematical expression of compaction of shales can be set up with consideration of time and depth, and the shale compaction curves can be drawn. The scatters of porosity-depth plots in term of different time sequences were revealed and the variations on compilation curves, e.g. Mondol, et al. (2007) in Fig. 3.1, can be classified by geological time sequences.

The meaning of the shale compaction can be simply described as the process which is compressed from mud into a clay and finally into a shale. The compaction is a burial diagenetic process to reduce porosity of shale partly or wholly caused by the gravitational loading. Generally, the compactions of shales have been known that mechanical compaction dominates in the shallow parts of the basin and chemical compaction dominates in the deeper parts of the basin.

The compilations of the shale compaction curves (Skemption, 1944; Engelhardt and Gaida, 1963; Miyazaki, 1966; Meade, 1966; Baldwin and Butler, 1985; Dzevanshir et al., 1986; Mondol et al., 2007) from several basins demonstrate variations and scattered data, especially at the shallow part of the basin in which mechanical compaction is dominance. For an example, Fig. 3.1 shows variations of shale compaction curves created by Mondol et al. (2007). The authors did not explain doubts of variation curves, and they did not show, however, a mathematical relationship between time (geological time) and porosity of shales. Hence, the variations of compaction curves on porosity-depth plots show that only mechanical compaction cannot explain the scattered data and variations of shale
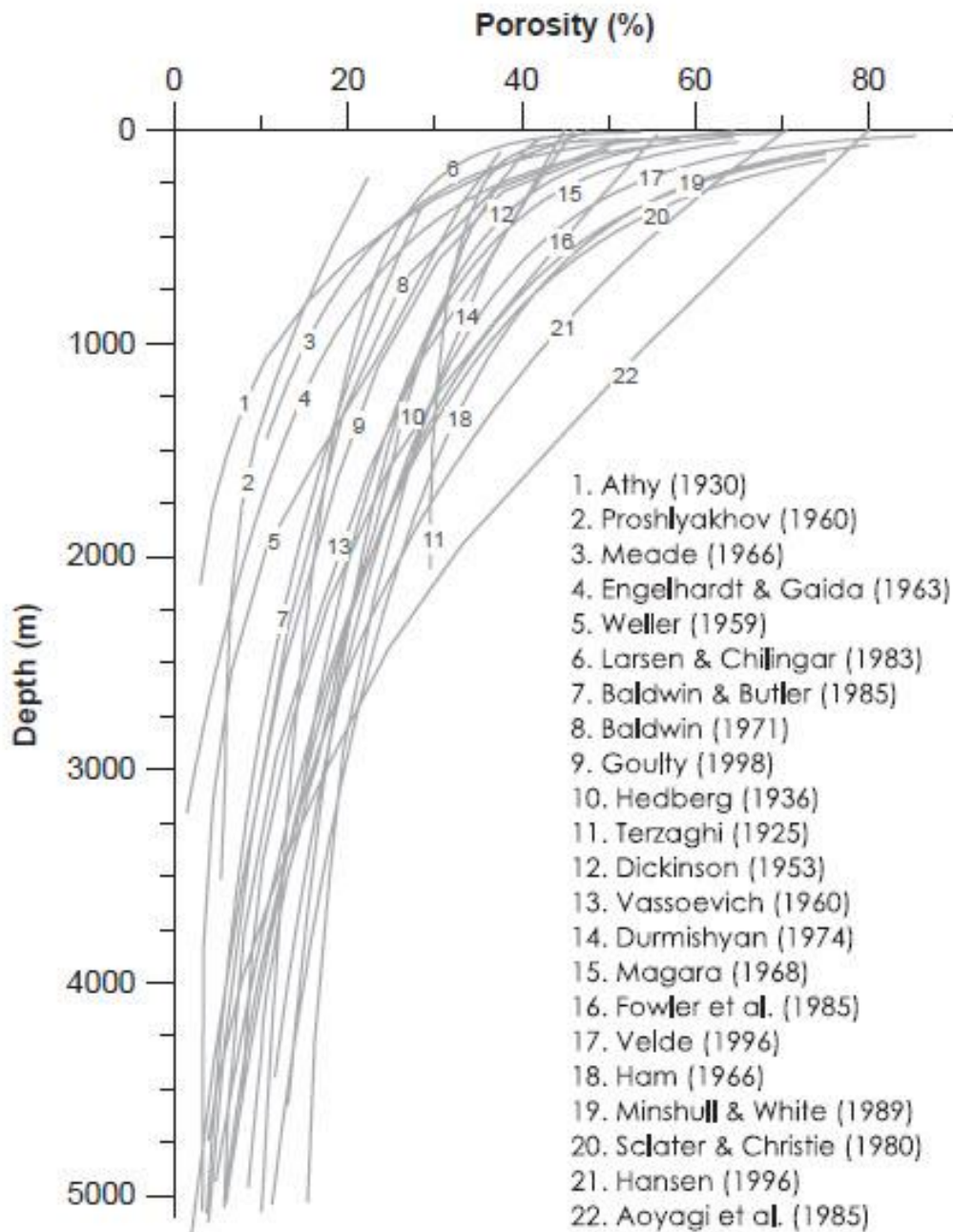
Fig. 3.1 Compilation curves of shale compactions (Mondol et al., 2007)

compaction curves.

Mechanical compaction is a type of the diagenetic processes in the compaction. The mechanical compaction can be described as a function of porosity, and controlled by overburden (i.e., burial depths), effective stress and pore pressure. The function has been proposed in term of porosity and burial depth based on both field observations and experimental studies. An empirical equation of compaction is practically expressed as an exponential function with a negative coefficient (Athy, 1930), and has been widely used for exploring the relationship of compaction of shale sediments (including shales). The porosity (ϕ) is expressed as a function of burial depth (z) as shown in Eq. (1). This model was derived from viewpoints of statistical physics by Korvin (1984).

$$\phi = \phi_0 e^{-az} \tag{1}$$

Where a is the constant representing localism environments of basins, and ϕ_0 is the initial porosity at a datum depth.

Nevertheless, porosity of shales at a depth is also determined by effective stress (σ_e). The same relationships of porosity and effective stress (Dutta, 2002; Flemings et al., 2002; Peng and Zhang, 2007, Zhang, 2011) can be established:

$$\phi = \phi_0 e^{-a\sigma_e} \tag{2}$$

The effective stress can be determined by total stress (σ_v) and pore pressure (P_p) that satisfy a famous equation as called Terzaghi's model. Following relationship (Terzaghi, 1925; Rubey and Hubbert, 1959):

$$P_p = \sigma_v - \sigma_e \tag{3}$$

where Biot coefficient (α) is normally assumed to be 1 (i.e., rock framework-grains are incompressible) and σ_v is normally known the overburden stress (total stress; here horizontal stress, normally of tectonic origin, is neglected).

Compaction of soils and clays has been described by Terzaghi's equation (Terzaghi, 1925, 1943). Terzaghi's equation includes time as one of variable parameters. This directly indicates effect of time on sediment compaction. To reveal the effect of time on shale compaction, it was assumed that conditions of compaction, i.e. permeability of sediments are much smaller, and changes of water saturation and relaxation of excess pressures due to changes of stress state take place much slower than in aquifer sediments. Water cannot migrate rapidly from one part to another (or adjacent more permeable layers that promote expulsion of excess water). This phenomenon produces a time lag between a change of forces that cause compaction and corresponding change of water saturation in sediments. The excess pressure (u), the pressure difference between the static and pore pressure, in the water contained in compacting beds of clay is a function of the time (t) and depth (z) as shown in Eq. (4), where c_{vc} is called that the coefficient of compaction.

$$\frac{\partial u}{\partial t} = c_{vc} \frac{\partial^2 u}{\partial z^2} \tag{4}$$

Following Terzaghi's assumptions for Eq. (4), i.e. 1) the process of consolidation proceeds very slowly, 2) the voids are completely filled with water, 3) the rocks are homogeneous and 4) only water moves in the framework, it can be rewriten the Eq. (4) using the porosity instead of the excess pressure as a function of time and depth of slow compaction following Fowler and Yang (1998)'s equation:

$$\frac{\partial \phi}{\partial t} = \lambda' \frac{\partial^2 \phi}{\partial z^2}, \quad \lambda' = \lambda \frac{(1-\phi_0)^2}{\phi_0} \tag{5}$$

$$\lambda = \frac{k_0}{M}, \quad k_0 = \frac{K_0 \gamma_w}{\mu} \qquad (6)$$

where λ is the compaction number, ϕ_0 is the initial porosity, M is the sedimentation rate, μ is the fluid viscosity, γ_w is the unit weight of water, K_0 is the initial permeability, and k_0 is the initial permeability coefficient.

4. Methodology

4.1 Re-construction porosity-time plots of Burst (1969)

Based on effect of time was re-studied and analyzed as shown in previous sections, the data plots on porosity-time modified from Burst (1969), as shown in Fig. 1.1, can be reproduced. Although Burst (1969)'s plots showed that the porosity of mudrocks tend to decline as a function of increasing time. However, his plot was not clear because he only plotted ranges of porosities with times, and depths (or age range of sample) were not specified, i.e. effect of time did not only influence on the decline of the porosity because mechanical compaction (burial depth) was still dominant.

Consequently, this section selected specific depths at 3000, 4000 and 5000 ft. (Meaning effective stress does not affect compaction processes at each depth) to reveal an effect of time, as shown in Fig. 4.1, and eventually found that porosity declines as a function of geologic time as same as Burst (1969).

4.2 Data Collection

Shale compaction data used in this study came from several sedimentary basins. The porosity and density are theoretically related and known as the indicators of the compaction of sediments. All data have no information on major erosions and unconformities. The data used in this study are listed in Table 4.1 along with basin location, bottom depth, porosity measurement, amount of data, and reference.

Fig. 4.2 represents varieties of basins of data that were used in this study. The geographic map shows that the data were taken by both onshore (Data No. 1, 3.7, 3.8, 4, 5, and 6) and offshore (Data No. 2, 3.1, 3.2, 3.3, 3.4, 3.5, and 3.6) basins, including Japan (No. 1 and 3.7), Gulf of Oman (No. 2), U.S.A. (No. 4), Venezuela (No. 5), Barbados (No. 3.2), Italy (No. 3.8), Antarctic Ocean (No. 3.3), Indian Ocean (No. 3.5), Pacific Ocean (No. 3.1), Philippines (No. 3.4), Atlantic Ocean (No. 3.6), and Northeastern Thailand (No. 6). The obtained data can be represented shale compaction data of around world. All amounts of data used are more than 850 data. The numbers on the geographic map are correlated the No. in the Table 4.1, which identify locations of basins.
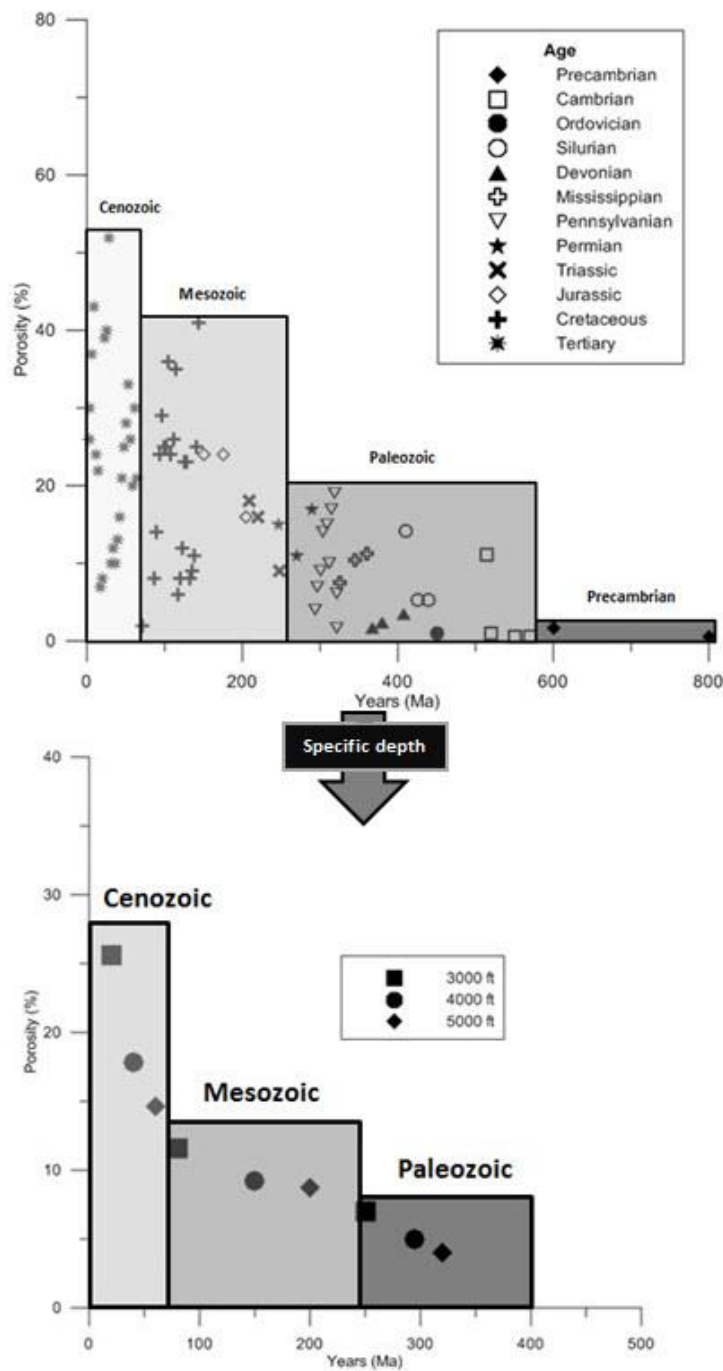
Fig. 4.1 Re-construction of porosity-geologic time plots from Fig. 1.1 (Burst, 1969)

4.2.1 Data Acquisition

The porosity data No. 1 were from the core samples obtained at 16 wells in Akita oil field, Japan. The natural densities of the samples were measured within a few hours, just after taken from wells, and then were converted to porosity data by that assuming specific gravity of the present sea water as 1.025, thus the average specific gravity of the grain is 2.65, as followed:

Table 4.1 Shale compaction data description

| No.	Basin location	Bottom depth (km)	Porosity Measurement	Amount of data	Reference
1	Akita	3.00	Direct measurement	143	Aoyagi *et al.* (1979; p.41)
2	Makran	5.00	Wireline measurement	25	Fowler *et al.* (1985; p.429-430)
3.1	N Pacific	0.05			
3.2	Barbados	0.46			
3.3	Antarctic	0.30			
3.4	Sulu Sea	1.00	Direct measurement	138	Velde (1996; p.196)
3.5	Indian Ocean	1.30			
3.6	E Atlantic	0.30			
3.7	Niigata	4.50			
3.8	Po Valley	2.50			
4	Oklahoma	2.00	Direct measurement	368	Athy (1930; p.12)
5	Maracaibo	2.00	Direct measurement	37	Hedberg (1936; p.254)
6	Northeastern Thailand	3.51	Wireline measurement	153	Department of Mineral Fuels, Thailand
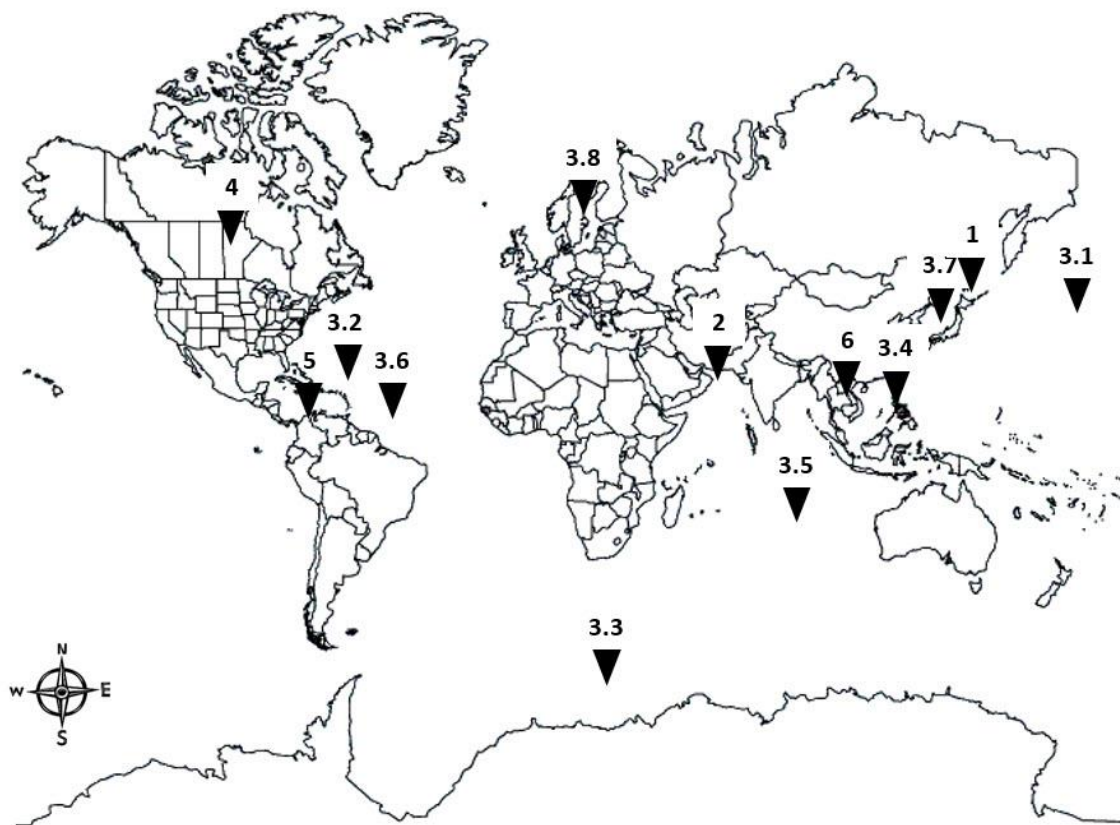
Fig. 4.2 Geographic map of data locations

$$\phi = \frac{\rho_g - \rho}{\rho_g - \rho_l} \tag{7}$$

where ρ is the natural density, ρ_g is the grain density, ρ_l is the density of pore water, and ϕ is the porosity.

For No. 2, porosity data were estimated by seismic velocity data using an empirical relationship derived by Hamilton (1978). First the seismic velocity was converted to bulk density (ρ_s), and then the bulk density was converted to porosity (ϕ) by using following equation:

$$\rho_S = \phi\rho_w + (1 - \phi)\rho_g \tag{8}$$

a grain density (ρ_g) of 2.762 g/cm^3 and a pore water density (ρ_w) of 1.050 g/cm^3 are assumed from measurements on Deep Sea Drilling Project (DSDP) site 222.

For group of data No. 3 (i.e. 3.1, 3.2, 3.3, 3.4, 3.5, 3.6, 3.7 and 3.8) the porosity data were obtained from several basins. Almost all data were taken from Ocean Drilling (ODP) and DSDP. The porosity data were acquired from consolidation test in laboratory. The laboratory test is for porosity measurements as a void ratio and the compacting force as pressure exerted by the solids. The porosity (ϕ) is related to void ratio (e) by Eq. (9).

$$e = \frac{\phi}{(1 - \phi)} \tag{9}$$

In cases of data No. 4 and 5, porosities were estimated from density data as followed:

$$\phi = \left[1 - \left(\frac{Bulk\ density}{Absolute\ density}\right)\right] \cdot 100 \tag{10}$$

where bulk density is the density of thoroughly dried rock, i.e. pore space free of liquids, and absolute density (or the so-called grain density) is the density of constituent particles of a rock, i.e. rock substance free from pore space (Hedburg, 1936). However, they are different way to obtain the density data. The bulk density of data No. 4 was acquired by weighing a sample in mercury with a Jolly balance and a sufficient mass being suspended to submerge the sample. While, the data No. 5 used Melcher method and pycnometer method in order to measure bulk density and absolute density, respectively. In addition, this study assumed the absolute density of data No. 4 remains constant and equal 2.762 g/cm^3 (Fowler et al., 1985) for calculating in Eq. (10).

Data No. 6 are the combination of shale data from several basins in the northeastern part of Thailand. The data were taken by density logging, sonic logging, and neutron logging. The porosity data were calculated by using Eq. (8) for density logging and Eq. (11) for sonic logging. The equation for calculating porosity from sonic

logging is shown as follows:

$$\phi = \frac{\Delta t - \Delta t_{ma}}{(\Delta t_f - \Delta t_{ma})} \tag{11}$$

where Δt is an acoustic transit time (μsec/ft), an acoustic transit time of water (Δt_f) is of 218 μsec/ft and an acoustic transit time of shale (Δt_{ma}) is assumend to be 62.5 μsec/ft.

4.2.2 Basin Information

The geologic information of data No. 1 referred to Miyazaki (1966). The samples were taken from Akita oil field and range from the shale of the Sasaoka formation to the black shale of the Funakawa formation. In fact, the density distribution on each well seems to be pretty normal. Each well is situated near the crest of gentle anticline, where can be recognized no structural disturbances in sediments.

While, the data No. 2 were taken from abyssal plain sediments in the Makran accretionary prism of northwest Indian Ocean. The oceanic Arabian plate is subducting shallowly northwards beneath the continental Eurasian plate. The abyssal plain sediments were stated that they are undeformed sediments and very little erosion takes place. According to they do not exhibit major internal deformation, thus they do not undergo tectonic consolidation.

Basin histories of group of data No. 3 stated that the samples were not affected by diagenesis and were critical to any interpretation of general sedimentary compaction phenomenon in ocean basins as it was the beginning stages of particle re-arrangement which must necessarily condition later stages of volume reduction which are only due to pressure.

The basin information of the Oklahoma basin in data No. 4 stated that all the samples studied were taken from areas of structural deformation and some of compaction may have resulted from vertical and lateral pressures in the earth's crust. The samples were acquired from wells in the Mervine, South Ponca, Thomas, Garber, and Blackwell fields. The sediments range from Permian age to base of Pennsylvanian age with no intervening unconformity.

Data No. 5 was obtained from the Geological Laboratory of Venezuela Gulf Oil Company. These data came from the study of core samples of Tertiary shales from wells drilled in the large geosynclinal basins of Venezuela. The samples were taken from a deep test in undisturbed and essentially horizontal Tertiary strata far removed from areas of major tectonic disturbance and the strata consisted in large part of shales which were free from appreciable sand impurity. In addition, absence of major unconformities in the section makes it possible to assume that the existing

overburdens are maximum overburdens.

Finally, the data No. 6 is shales in the northeastern part of Thailand. The shales are locally thick, organic-rich, dry gas prone, deeply buried, and overpressured. They was initiated during the Middle Paleozoic, with widespread deposition of clastic and carbonate sedimentary rocks. Tectonic extension during the Early Permian broke the basin apart into numerous horst and graben blocks separated by high-angle normal faults.

4.3 Data Analysis

Assembled data were plotted on porosity-depth relationship as shown in Fig. 4.3, and then the specific depths (500 and 1,500 m) were mentioned to show that mechanical compaction (burial depth or effective stress is kept constant in order to ignore depth effect) is certainly one of the main controlling factors of compaction of shales, but porosity still declines even mechanical compaction (burial depth or effective stress is kept constant as the depth at 500 and 1,500 m) does not influence on compactions.

Furthermore, the factors that influence on shale compaction are shown in Table 4.2. Those factors are basin type, lithology, thickness of strata, age of stratum and compaction factors. The compaction factors, i.e. porosity of shaee at datum depth (ϕ_0) and constant value of exponential function (a), were determined by fitting curves of Eq. (1).

Table 4.2 revealed that the variations of compaction curves of shales can be due to several factors and the compaction is affected by several factors which control compaction under localized environments. Time (or geologic age) is likely to be a major factor that influences variations of compaction processes of shales. It is because the coefficients of compactions show an increasing tendency with increasing time in the summary table.

Table 4.2 Shale compaction data analysis

| No.	Basin location	Basin type	Lithology	Thickness of strata (km)	Age of stratum	Compaction factor	
						ϕ_0 (%)	a (km^{-1})
1	Akita and Hokkaido	Back-arc	Black shale	0.2 - 3	Mio-Cretaceous	72	0.656
2	Makran	Abyssal	Silt and Clay sediment	0 - 5	Paleo-Neogene	54	0.476
3.1	N Pacific	Deep-water	Clay-rich sediment	0.05 - 4	Pleistocene	56	0.486
3.2	Barbados				Eo-Holocene		
3.3	Antarctic				Plio-Pleistocene		
3.4	Sulu Sea				Mio-Pleistocene		
3.5	Indian Ocean				Paleo-Neogene		
3.6	E Atlantic				Plio-Holocene		
3.7	Niigata	Back-arc and Convergent			Mio-Holocene		
3.8	Po Valley				Plio-Holocene		
4	Oklahoma	Convergent	Red shale	0.5 - 2	Perm-Penn	36	1.006
5	Maracaibo	Back-arc	Greenish gray mud	0.08 - 2	Paleo-Neogene	41	0.698
6	Northeastern Thailand	Fluvial and Lacustrine	Organic-rich shale	0.2-3.5	Carbo-Triassic	8.75	0.071
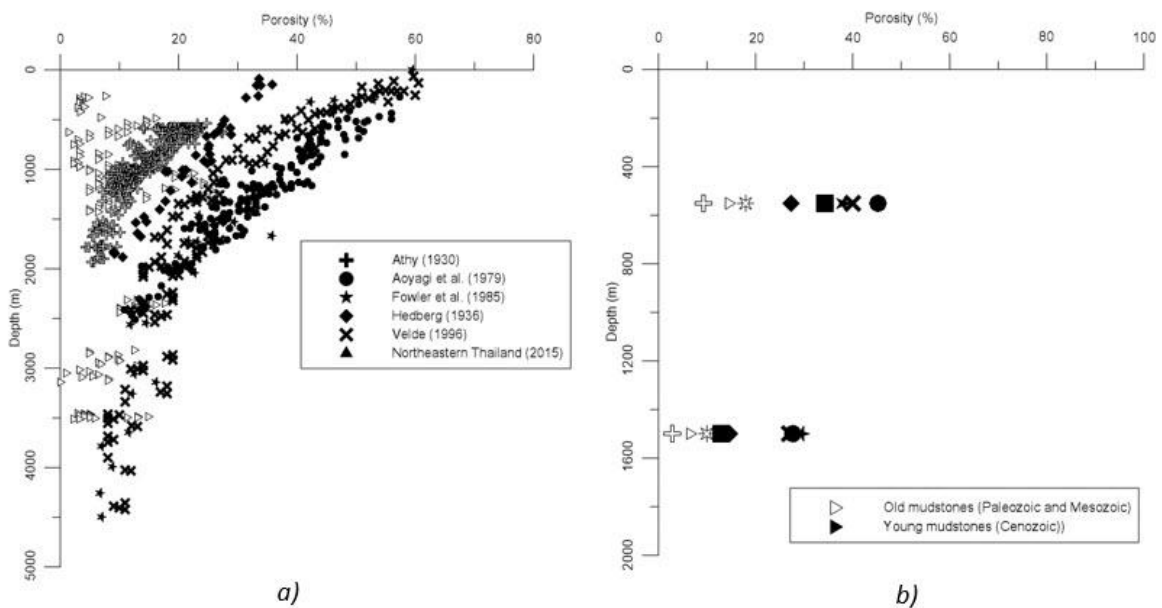
Fig. 4.3 Data plots of different times on porosity-depth relationship *a)* Scattered data on shale compactions *b)* Depth specifications (at depth 500 and 1,500 m) revealing effect of time

4.4 Construction of Mathematic Equation on Time Effect of Shale Compaction

Based on Terzaghi's equation and assumptions (Terzaghi, 1925, 1943) as shown in Eq. (4) and Fowler and Yang (1998)'s equation in Eq. (5) and (6). To reveal the effect of time on shale compactions, a mathematical expression of compaction of shales considering both time and depth was established (Eq. (12)), and it also shows

that if time factor is omitted, Eq. (12) will be reduced to Athy's model as shown in an Eq. (1) (This study ignored mutual dependence of z and t in a geological process). An actual set of data from a well represents geological processes and histories of the stratigraphic succession pass through. Hence, as long as this study stick to the actual data, the ignorance of mutual dependence of z and t can be implicitly expressed in analysis of the actual data based on Eq. (12) is cancelled in an evaluation of constants ϕ_0 and a, etc.

$$\phi(z, t) = \phi_0 e^{-(az + a^2 \lambda' t)} \tag{12}$$

where λ is the compaction number, ϕ_0 is the initial porosity.

4.5 Shale Compaction Curves Considering with Time Effect

The theoretical parameters of the shale compaction are listed in Table 4.3; they are initial porosity (ϕ_0) which was reported that the surface porosity of shales range around 60 – 65 %, initial permeability (K_0), fluid viscosity (μ), and unit weight of water (γ_w) were used by the standard numbers of mudstones and water, the sedimentation rate (M) was assumed for slow compaction model of shale compaction, and constant value of exponential function (a) which was obtained by an average of constant values of exponential function from several published compaction curves. By using those parameters based on geological consideration for various basins used in Eq. (12). Shale compaction curves varying with times from 0 to 550 Ma (Cenozoic to early Paleozoic age) can be drawn as shown in Fig. 4.4.
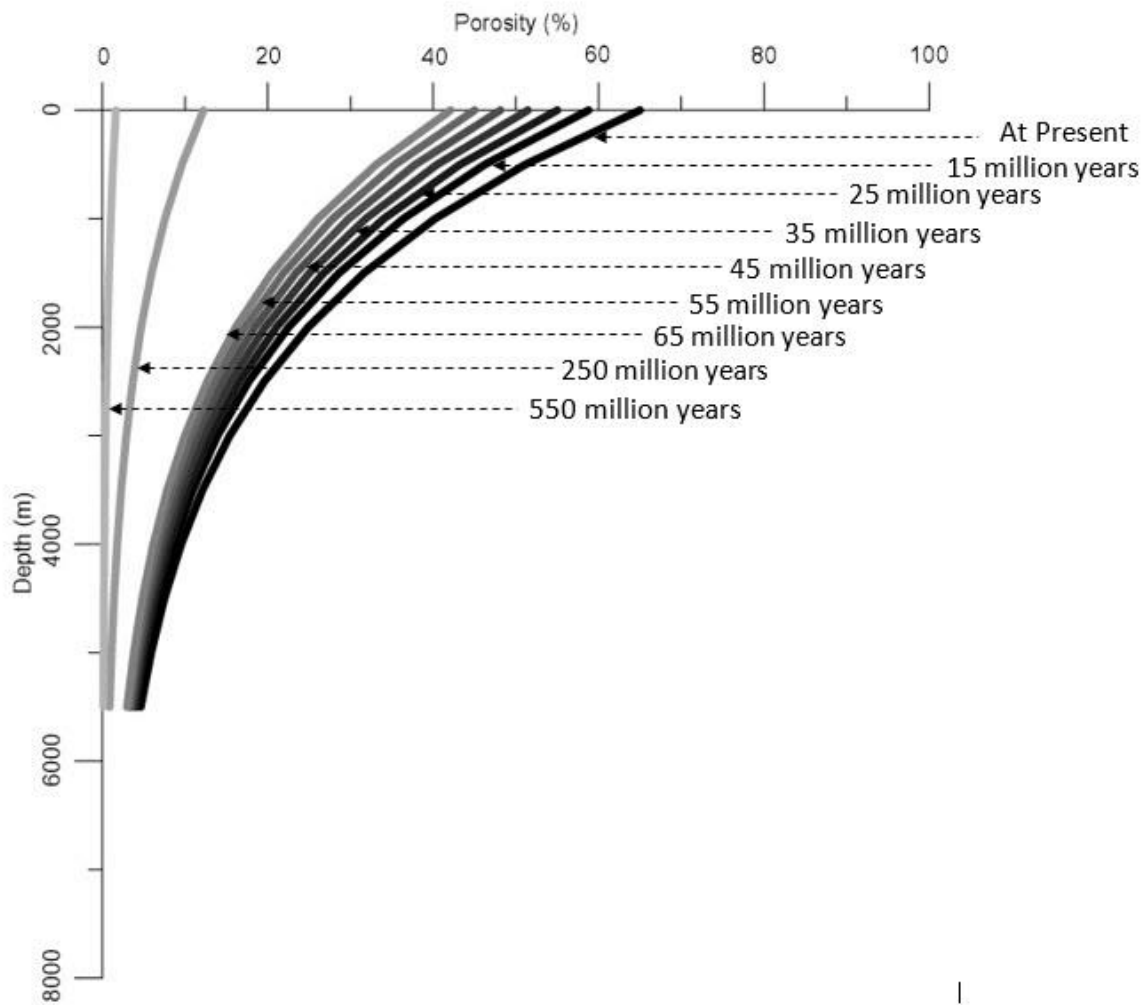
Fig. 4.4 Shale compaction curves considering with time effect

Table 4.3 Assuemed parameters for mudstone compaction curves varying with time

Parameters	Value	Unit
Constant value of exponential function (a)	0.48	Km^{-1}
Initial porosity (ϕ_0)	65	%
Unit weight of water (γ_w)	1x10^4	N/m^3
Initial permeability (K_0)	0.38	μD
Fluid viscosity (μ)	0.8x10^{-3}	Pa·s
Sedimentation rate (M)	1	mm/yr

5. Result and Discussion

5.1 Shale Compaction Curves Considering with Time Effect on Data Plots

The shale compaction curves considering with time effect plots with actual data are shown in Fig. 5.1. The graph shows an acceptable match between compaction curves and actual data based on time variations. The scattering of actual data from Cenozoic age to middle time of Paleozoic age can also be explained as effect of time on shale compactions, but this study used assumed parameters to constrain only time factor influences on shale compactions. The order of 100 million years is necessary for us to recognize clearly the effect of time on shale compaction.
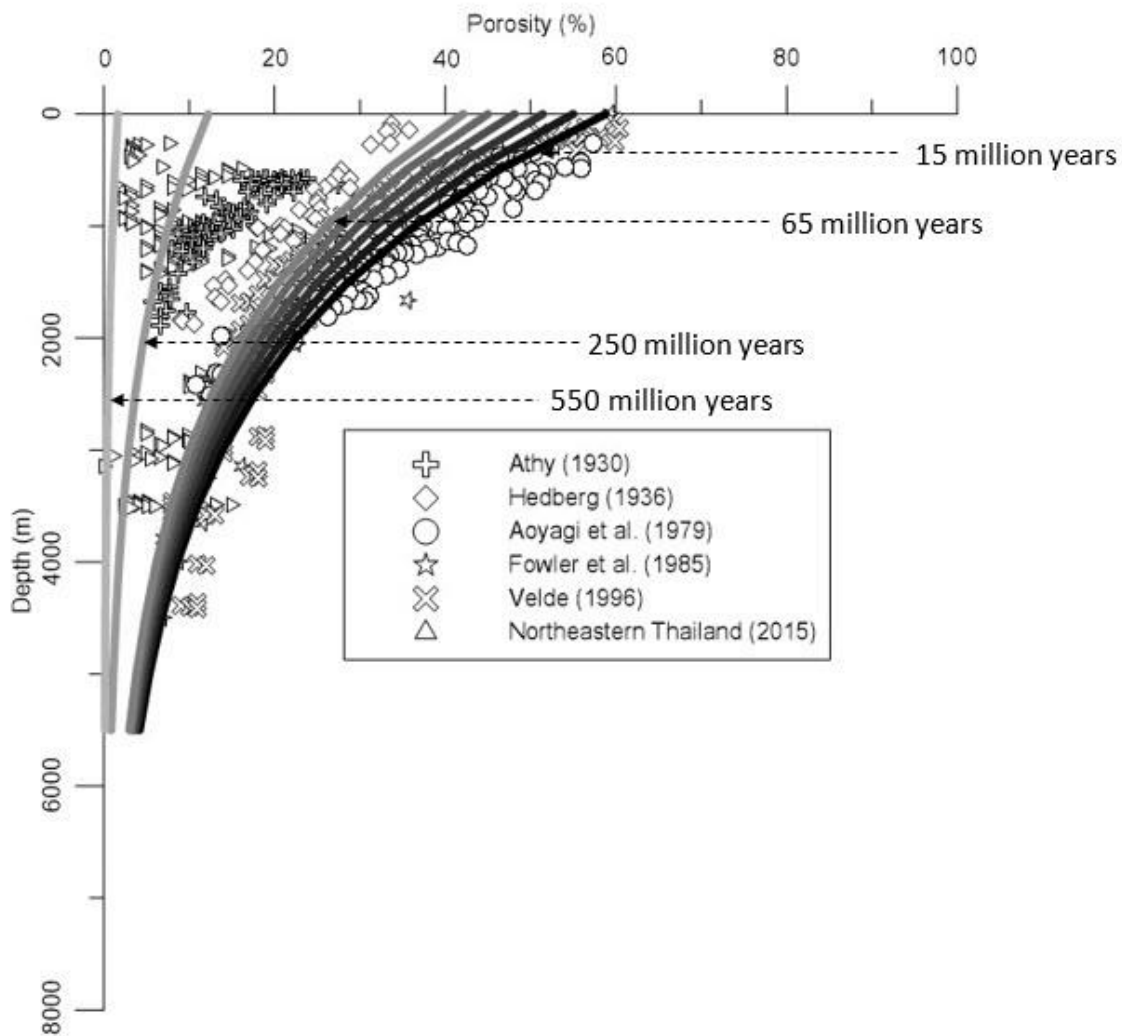

Fig. 5.1 Shale compaction curves considering with time effect on observed data

5.2 Time Effect Model Verification by 3D Plots

In this section, the data of porosity, depth and time were plotted on 3D graph, as shown in Fig. 5.2, in order to determine matching between shale compaction

modle considering with time effects (Eq. (12)) and actual data on 3D-plots. The porosity data were transformed by natural logarithm, while the time data were plotted in ranges of geologic times. The plane fitting of the data is in accord with mathematic model of time effect (Eq. (12)) in natural logarithm function as shown in Eq. (13).

$$ln\, \phi = \, ln\, \phi_0 - az - a^2 \lambda' t \qquad (13)$$

Fig. 5.2 shows that the data could be fitted by plane fitting ($R^2 = 0.7$) of Eq. (13). This can explain the mathematic model that has been setup in this chapter can use and represent compaction data considering with time effect, and it can confirm that the mathematic model which has been setup in exponential function corresponding with function among porosity, depth, and time.

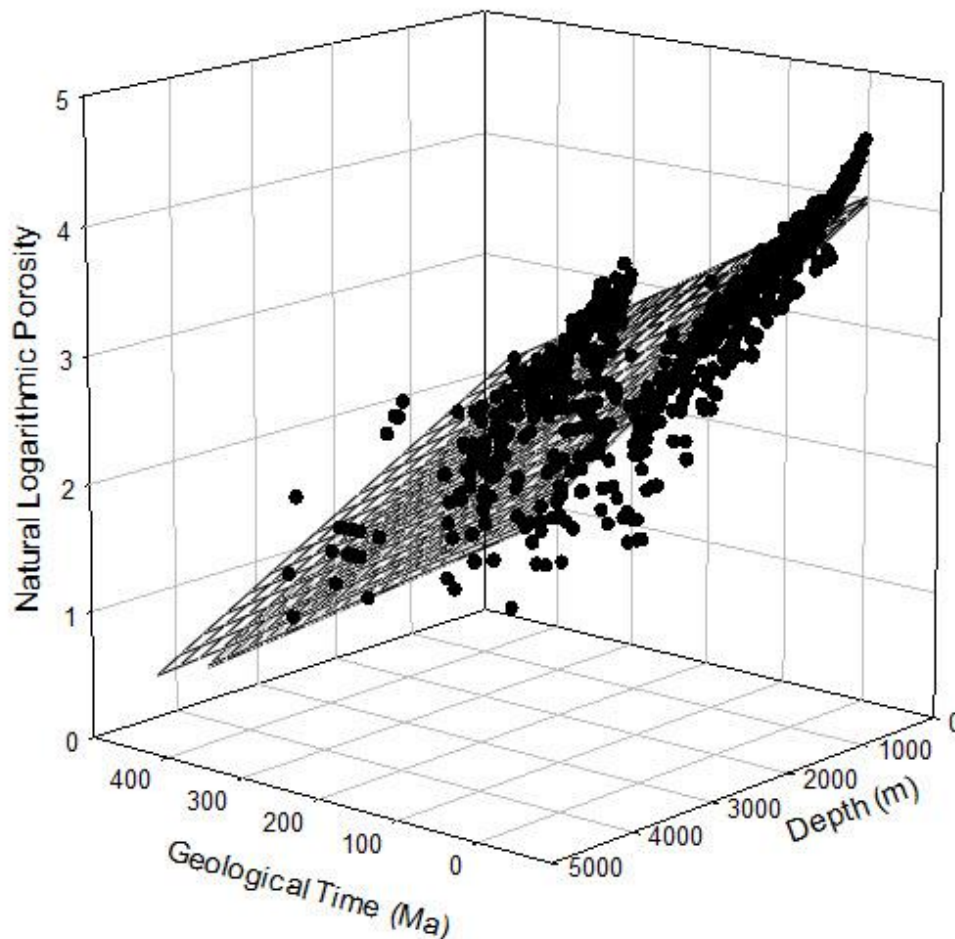
Porosity-Depth-Geological Time Plots

Table 5.1 Comparison between assumed and calculated parameters

Parameters	Theoretical value	Calculated value	Unit
Constant value of exponential function (a)	0.48	0.40	Km^{-1}
Initial porosity (ϕ_0)	65	51.5	%
Initial permeability (K_0)	0.38	0.13	μD
λ'	0.029	0.024	-

The parameters were determined by least square method of 3D plots, so the calculated parameters of compaction, i.e. initial porosity (ϕ_0), initial permeability (K_0), constant value of exponential function (a) and λ', were calculated to verify with theoretical parameters (used for setting up mathematic model of shale compaction considering with time effect) as shown in Table 5.1.

The comparisons show that the calculated parameters from 3D plots are consistent with assumed (or theoritical) parameters; it means that the property and condition, which were assumed in order to calculate and draw shale compaction curves considering with time effects, were satisfactorily reasonable and can be represented to demonstrate effect of time on shale compactions.

6. Conclusion

Compaction of shales is defined as a function of porosity, and has been described in a burial diagenetic process to reduce porosity of shales. Mechanical process is the main among factors controlling the compaction, and is controlled mainly by overburden (i.e., burial depths), effective stress and pore pressure. This study revealed that mechanical compaction (or burial depths) is certainly one of the main controlling factors of compaction of shales, but it cannot be a single factor to explain the relationship between porosity of shales and burial depths in a form of a compaction curve. The time effect can be observed clearly in scale of 100 million years. This work analyzed and classified effects of several factors, i.e. basin type, lithology, geologic age or time, thickness, etc (as shown in Table 4.2). Such compaction factors, influencing scatters of data points from a normal trend, cause variations of shale compaction curves.

Time is an important factor to influence the compaction as well as overburden. Time after deposition of mud promotes its compaction. Effect of geological time on the compaction is far more difficult for us to analyze than overburden. It is because an experiment is impossible for geological time. Results of analysis of Table 3.3 and Fig. 4.3 show that time (or age) is likely to be an effective factor influencing variations of compaction processes of shales. In addition, this study re-evaluated on time effect of mudrock compactions based on theory of consolidation (Terzaghi equation) proposed by Terzaghi (1925, 1943). Assuming the processes of compactions are very slow (compaction number, $\lambda < 1$), shales have low permeability, and the rock model is a homogeneous following Terzaghi's assumptions, and thus a differential equation of excess pore pressure considering with time and depth proposed by Terzaghi (1925, 1943) can be replaced by slow compaction model of Folwer and Yang (1998)'s differential equation.

A mathematical expression of compaction of shales can be set up with consideration of time and depth, and the shale compaction curves can be drawn. The scatters of porosity-depth plots in term of time effect were revealed and the variations on compilation curves of Mondol et al. (2007) can be classified by time effect. Finally, this study furnished results of Dzevanshir et al. (1986) and supported that time factor should be paid more attention on mechanism of mudstone compaction. Furthermore, this study can also help us to understand the mechanism of shale compaction, especially at the shallow part that is dominated by the mechanical compaction.

Reference

Athy, L.F., 1930. Density, porosity, and compaction of sedimentary rocks. American Association of Petroleum Geologists Bulletin, 14 (1): 1-24.

Baldwin, B. and Butler, C.O., 1985. Compaction curves. American Association of Petroleum Geologists Bulletin, 69: 622-626.

Burst, J.F., 1969. Diagenesis of gulf coast clayey sediments and its possible relation to petroleum migration. American Association of Petroleum Geologists, 53 (1): 73-93.

Dutta, N.C., 2002. Geopressure prediction using seismic data: current status and the road ahead. Geophysics, 67: 2012-2041.

Dzevanshir, R.D., Buryakovskiy, L.A., and Chilingarian, G.V., 1986. Simple quantitative evaluation of porosity of argillaceous sediments at various depths of burial. Sedimentary Geology, 46: 169-175.

Engelhardt, W.V., and Gaida, K.H., 1963. Concentration changes of pore solutions during the compaction of clay sediments. Journal of Sedimentary Petrology, 33 (4): 919-930.

Flemings, P.B., Stump, B.B., Finkbeiner, T., Zoback, M., 2002. Flow focusing in overpressured sandstones: theory, observations, and applications. American Journal of Science, 302: 827-855.

Fowler, A.C. and Yang, X.S., 1998. Fast and slow compaction in sedimentary basins. SIAM Journal on Applied Mathematics, 59, (1): 368-385.

Fowler, S.R. White, R.S., Louden, K.E., 1985. Sediment dewatering in the Makran accretionary prism. Earth and Planetary Science Letters, 75 (4): 427-438.

Hamilton, E.L., 1978. Sound velocity-density relations in sea-floor sediments and rocks. The Journal of the Acoustical Society of America, 63: 366-377.

Hedberg, H.D., 1936. Gravitational compaction of clays and shales. American Journal of Science, 31 (184): 241-287.

Korvin, G., 1984. Shale compaction and statistical physics. Geophysical Journal International, 78: 35-50.

Manger, G.E., 1963. Porosity and bulk density of sedimentary rocks. United States Geological Survey, 1144-E: 34-40.

McCoy, A.W. and Keyte, W.R., 1934. Present interpretations of the structural theory for oil and gas migration and accumulatlion. Problem of Petroleum Geology (Sidney Powers Memorial Volume), American Association of Petroleum Geologists, Tulsa, Oklahoma: 279-282.

Meade, R.H., 1966. Factors influencing the early stages of the compaction of clays and sands-review. Journal of Sedimentary Petrology, 36 (4): 1085-1101.

Miyazaki, H., 1966. Gravitational compaction of the Neogene muddy sediments in Akita oil fields, northeast Japan. Journal of Geosciences, Osaka City Univ., 9: 1-23.

Mondol, N.H., Bjorlykke, K., Jahren, J., Hoeg, K., 2007. Experimental mechanical compaction of clay mineral aggregates-Changes in physical properties of mudstones during burial. Marine and Petroleum Geology, 24: 289-311.

Peng, S. and Zhang, J., 2007. Engineering geology for underground rocks. Springer.

Rubey, W.W. and Hubbert, M.K., 1959. Role of fluid pressure in mechanics of overthrust faulting. II. Overthrust belt in geosynclinals area of western Wyoming in light of fluid-pressure hypothesis. Geological Society of America, 70 (2): 167-205.

Skempton, A.W., 1944. Notes on the compressibility of clays. Quarterly Journal of the Geological Society, c: 119-135

Terzaghi, K., 1925. Erdbaumechanik. Deuticke, Vienna. (Casagrande, A., translated, 1960; From Theory to Practice in Soil Mechanics; selections from the writings of Karl Terzaghi, with bibliography and contributions on his life and achievents). NY, John Wiley and Sons: 425pp.

Terzaghi, K., 1943. Theoretical of soil mechanics. John Wiley and Sons: 510 pp.

Van Olphen, H., 1963. Compaction of clay sediments in the range of molecular particle distances, in Clays and clay minerals. 11th Natl. Clays and Clay Mineral Conference Proceeding, New York, Macmillan Co.: 178-187

Velde, B., 1996. Compaction trends of clay-rich deep sea sediments. Marine Geology, 133 (3-4): 193-201.

Versluys, J., 1927. A hypothesis explaining some characteristics of clay. Proc. Konink. Akad. Van Wetenschappen te Amsterdam, 30: 104-112.

Weatherby, B.B. and Faust, L.Y., 1935. Influence of geological factors on longitudinal seismic velocities. American Association of Petroleum Geologists, 19: 1-8.

Zhang, J., 2011. Pore pressure prediction from well logs-Methods, modifications, and new approaches. Earth-Science Reviews, 108: 50-63.